

Axial Ligand Modulation of the Electronic Structures of Binuclear Copper Sites: Analysis of Paramagnetic ^1H NMR Spectra of Met160Gln Cu_A

Claudio O. Fernández,[†] Julia A. Cricco,[‡] Claire E. Slutter,[§] John H. Richards,[§] Harry B. Gray,[§] and Alejandro J. Vila^{*,‡}

Contribution from the Biophysics Section, University of Rosario, Suipacha 531, S2002LRK Rosario, Argentina, LANAIS RMN-300 (University of Buenos Aires-CONICET), Junín 956, C1113AAD Buenos Aires, Argentina, and Beckman Institute and Division of Chemistry and Chemical Engineering, California Institute of Technology, Pasadena, California 91125

Received May 22, 2001

Abstract: Cu_A is an electron-transfer copper center present in heme-copper oxidases and N_2O reductases. The center is a binuclear unit, with two cysteine ligands bridging the metal ions and two terminal histidine residues. A Met residue and a peptide carbonyl group are located on opposite sides of the Cu_2S_2 plane; these weaker ligands are fully conserved in all known Cu_A sites. The Met160Gln mutant of the soluble subunit II of *Thermus thermophilus* ba_3 oxidase has been studied by NMR spectroscopy. In its oxidized form, the binuclear copper is a fully delocalized mixed-valence pair, as are all natural Cu_A centers. The faster nuclear relaxation in this mutant suggests that a low-lying excited state has shifted to higher energies compared to that of the wild-type protein. The introduction of the Gln residue alters the coordination mode of His114 but does not affect His157, thereby confirming the proposal that the axial ligand-to-copper distances influence the copper–His interactions (Robinson, H.; Ang, M. C.; Gao, Y. G.; Hay, M. T.; Lu, Y.; Wang, A. H. *Biochemistry* **1999**, *38*, 5677). Changes in the hyperfine coupling constants of the Cys $\beta\text{-CH}_2$ groups are attributed to minor geometrical changes that affect the Cu–S–C $_{\beta}$ –H $_{\beta}$ dihedral angles. These changes, in addition, shift the thermally accessible excited states, thus influencing the spectral position of the Cys $\beta\text{-CH}_2$ resonances. The Cu–Cys bonds are not substantially altered by the Cu–Gln160 interaction, in contrast to the situation found in the evolutionarily related blue copper proteins. It is possible that regulatory subunits in the mitochondrial oxidases fix the relative positions of thermally accessible Cu_A excited states by tuning axial ligand interactions.

Introduction

The *caa_3* and *ba_3* cytochrome *c* oxidases are expressed by the thermophilic eubacterium *Thermus thermophilus* HB8 (ATCC 27634).^{1,2} Both enzymes are more promiscuous than the mitochondrial *aa_3* oxidases, displaying notable nitric oxide (NO) reductase activity.³ Kinetics studies³ nicely complement earlier sequence homology analysis predicting that the heme-copper oxidases and NO reductases evolved from a common ancestor and share similar reaction mechanisms.^{4,5} The *ba_3* oxidase, expressed under low O_2 -tension growth conditions,² is the smallest known cytochrome *c* oxidase (~85 kDa, 764 residues);⁶ it couples the four-electron reduction of O_2 to proton pumping across the membrane with only two subunits and an

additional transmembrane helix, designated subunit IIa.⁷ Subunit I contains a low-spin heme *b* and a heme *a*₃– Cu_B active site where O_2 or NO is reduced. Subunit II contains a solvent-exposed domain with a binuclear Cu_A center and an adjacent binding site for reduced cytochrome *c*₅₅₂. Compared to the *aa_3* oxidases, *ba_3* displays several distinct features, including slow O_2 turnover, reduced affinity for CO and CN^- ,⁸ reduced proton pumping efficiency [$0.4\text{--}0.5 \text{H}^+/\text{e}^-$],⁹ unusual heme reduction potential cooperativity,¹⁰ and a hydrophobic interaction with cyt *c*₅₅₂.⁸

Crystal structures of the *T. thermophilus* *ba_3* oxidase,⁶ its substrate cyt *c*₅₅₂,¹¹ and the soluble Cu_A domain of subunit II from *ba_3*¹² are available at 2.4, 1.28, and 1.6 Å resolution, respectively, providing a sound structural basis for examination of the Cu_A center. Soulimane et al.⁶ have proposed a direct electron transfer (ET) pathway between Cu_A and the heme *a*₃–

[†] University of Buenos Aires.

[‡] University of Rosario.

[§] California Institute of Technology.

(1) Fee, J. A.; Choc, M. G.; Findling, K. L.; Lorence, R.; Yoshida, T. *Proc. Natl. Acad. Sci. U.S.A.* **1980**, *77*, 147.

(2) Zimmermann, B. H.; Nitsche, C. I.; Fee, J. A.; Rusnak, F. M.; Munck, E. *Proc. Natl. Acad. Sci. U.S.A.* **1988**, *85*, 5779.

(3) Giuffrè, A.; Stubaer, G.; Sarti, P.; Brunori, M.; Zumft, W. G.; Buse, G.; Soulimane, T. *Proc. Natl. Acad. Sci. U.S.A.* **1999**, *96*, 14718.

(4) van der Oost, J.; de Boer, A. P.; de Gier, J. L.; Zumft, W. G.; Stouthamer, A. H.; Van Spanning, R. J. *FEMS Microbiol. Lett.* **1994**, *121*, 1.

(5) Saraste, M.; Castresana, J. *FEBS Lett.* **1994**, *341*, 1.

(6) Soulimane, T.; Buse, G.; Bourenkov, G. P.; Bartunik, H. D.; Huber, R.; Than, M. E. *EMBO J* **2000**, *19*, 1766.

(7) Soulimane, T.; Than, M. E.; Dewor, M.; Huber, R.; Buse, G. *Protein Sci.* **2000**, *9*, 2068.

(8) Giuffrè, A.; Forte, E.; Antonini, G.; D'Itri, E.; Brunori, M.; Soulimane, T.; Buse, G. *Biochemistry* **1999**, *38*, 1057.

(9) Kannt, A.; Soulimane, T.; Buse, G.; Becker, A.; Bamberg, E.; Michel, H. *FEBS Lett.* **1998**, *434*, 17.

(10) Hellwig, P.; Soulimane, T.; Buse, G.; Mantele, W. *Biochemistry* **1999**, *38*, 9648.

(11) Than, M. E.; Hof, P.; Huber, R.; Bourenkov, G. P.; Bartunik, H. D.; Buse, G.; Soulimane, T. *J. Mol. Biol.* **1997**, *271*, 629.

(12) Williams, P. A.; Blackburn, N. J.; Sanders, D.; Bellamy, H.; Stura, E. A.; Fee, J. A.; McRee, D. E. *Nat. Struct. Biol.* **1999**, *6*, 509.

Cu_B center that involves a ~ 10 Å tunneling step. A similar pathway has been proposed for the *aa*₃ oxidases,^{13,14} but kinetics studies are consistent with a Cu_A \rightarrow heme *a* \rightarrow heme *a*₃-Cu_B sequence in the *aa*₃ enzymes.¹⁵ The heme *a/b* center is believed to be critical for the coupling of ET to proton pumping in the oxidases. Consequently, an ET heme *b* bypass pathway in *ba*₃ may be used⁶ when an alternate terminal electron acceptor is unable to provide the driving force requirements for proton pumping. Thus, the primary function of the *ba*₃ oxidase may be to provide a terminal electron acceptor under very harsh conditions.

Disruption of the Cu_A center by the axial ligand mutation Met263Leu in the *Rhodobacter sphaeroides* *aa*₃ oxidase blocks Cu_A \rightarrow heme *a* ET without inhibiting proton uptake.¹⁶ This observation corroborates previous electronic structure calculations suggesting that axial ligand mediated modulation of the Cu_A Cu-S core is well suited as a control center for ET.¹⁷ Indeed, understanding axial structural perturbations of the Cu_A core could well reveal the role that this center plays in controlling ET during the oxidase reaction cycle.

Cu_A naturally exists in two redox states: in the reduced form, both metal atoms are cuprous ions, whereas, as originally inferred from the seven-line pattern in the EPR spectrum of N₂O reductase,¹⁸ the oxidized form is a fully delocalized class III mixed-valence pair.¹⁹ The binuclear assignment was later confirmed by crystal structure analyses of the engineered *E. coli* CyoA soluble fragment of cytochrome *bo*,²⁰ bovine *aa*₃ cytochrome *c* oxidase,^{13,13,21} and the bacterial *aa*₃ enzyme from *Paracoccus denitrificans*.¹⁴ Other structures recently have become available, notably from *Pseudomonas stutzeri* N₂O reductase²² and an engineered purple azurin.²³

The Cu_A center consists of an almost planar Cu₂S₂ core (Figure 1). In the Cu_A subunit from *T. thermophilus* *ba*₃ oxidase, the copper ions are bridged by the sulfur atoms of Cys149 and Cys153, forming an almost planar Cu₂S₂ rhombic structure with a metal-to-metal distance of 2.5 Å.¹² One of the coppers also binds the N δ 1 atom of His114 and the S δ of Met160 (at 2.48 Å), with a distorted tetrahedral geometry, whereas the other copper coordinates to His157 and the backbone carbonyl of Gln151 (at 2.62 Å). These structural features are largely conserved in natural and engineered Cu_A centers.

Magnetic spectroscopic methods such as EPR, MCD, and ENDOR have played a major role in the study of Cu_A sites.^{17,18,24-27} Historically, copper(II) sites in proteins have not

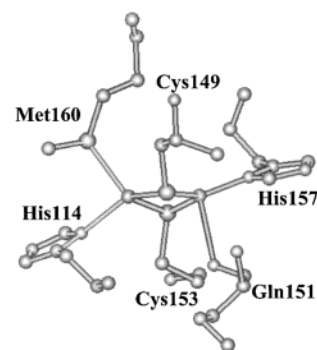


Figure 1. Schematic representation of the Cu_A site in the *T. thermophilus* fragment, as taken from the coordinates deposited in the PDB as 2cua.¹² Residue numbering corresponds to the full subunit II fragment.

been amenable to paramagnetic NMR studies because of an unfavorable electron relaxation time ($\sim 10^{-9}$ s) that leads to broad NMR lines.^{28,29} However, the unpaired electron in Cu_A sites relaxes considerably faster ($\sim 10^{-11}$ s),³⁰ giving rise to well-resolved ^1H NMR spectra.³¹ Since the initial report of the NMR spectrum of the Cu_A-containing soluble fragment of *T. thermophilus* cytochrome *ba*₃ (TtIICu_A),³² other results have become available.³³⁻³⁷ The anomalous temperature dependence of some of the resonances corresponding to the Cys ligands has been attributed to the existence of low-lying excited states that become populated at room temperature.³⁵ NMR has proven to be a particularly sensitive technique, because quite different signal patterns are observed for Cu_A centers displaying almost identical EPR and electronic spectra.

Several structures are now available for different oxidation and ligand-binding states of the bovine and *Paracoccus denitrificans* *aa*₃ oxidases. These structures reveal that the Cu_A center is structurally robust,^{6,12-14,21} suggesting that the mode of tuning the ET properties is subtle. The Met160Gln axial ligand has been successfully mutated in the *Thermus* *ba*₃ Cu_A soluble fragment, giving rise to stable binuclear mixed-valence centers, but with slightly altered EPR and UV-vis features.³⁸ Larger copper hyperfine interactions in the Met160Gln and Met160Glu mutants indicate that electron spin density has shifted from the ligands to the Cu nuclei, which in turn suggests that significant

(13) Tsukihara, T.; Aoyama, H.; Yamashita, E.; Tomizaki, T.; Yamaguchi, H.; Shinzawa-Itoh, K.; Nakashima, R.; Yaono, R.; Yoshikawa, S. *Science* **1996**, *272*, 1136.

(14) Iwata, S.; Ostermeier, C.; Ludwig, B.; Michel, H. *Nature* **1995**, *376*, 660.

(15) Winkler, J. R.; Malmström, B. G.; Gray, H. B. *Biophys. Chem.* **1995**, *54*, 199.

(16) Karpefors, M.; Adelroth, P.; Zhen, Y.; Ferguson-Miller, S.; Brzezinski, P. *Proc. Natl. Acad. Sci. U.S.A.* **1998**, *95*, 13606.

(17) Gamelin, D. R.; Randall, D. W.; Hay, M. T.; Houser, R. P.; Mulder, T. C.; Canters, G. W.; De Vries, S.; Tolman, W. B.; Solomon, E. I. *J. Am. Chem. Soc.* **1998**, *120*, 5246.

(18) Kroneck, P. M. H.; Antholine, W. E.; Riester, J.; Zumft, W. G. *FEBS Lett.* **1988**, *242*, 70.

(19) Robin, M.; Day, P. *Adv. Inorg. Chem.* **1967**, *10*, 247.

(20) Wilmanns, M.; Lappalainen, P.; Kelly, M.; Sauer-Eriksson, E.; Saraste, M. *Proc. Natl. Acad. Sci. U.S.A.* **1995**, *92*, 11955.

(21) Tsukihara, T.; Aoyama, H.; Yamashita, E.; Tomizaki, T.; Yamaguchi, H.; Shinzawa-Itoh, K.; Nakashima, R.; Yaono, R.; Yoshikawa, S. *Science* **1995**, *269*, 1071.

(22) Brown, K.; Tegoni, M.; Prudencio, M.; Pereira, A. S.; Besson, S.; Moura, J. J.; Moura, I.; Cambillau, C. *Nat. Struct. Biol.* **2000**, *7*, 191.

(23) Robinson, H.; Ang, M. C.; Gao, Y. G.; Hay, M. T.; Lu, Y.; Wang, A. H. *Biochemistry* **1999**, *38*, 5677.

(24) Antholine, W. E.; Kastrau, D. H. W.; Steffens, G. C. M.; Buse, G.; Zumft, W. G.; Kroneck, P. M. H. *Eur. J. Biochem.* **1992**, *209*, 875.

(25) Gurbiel, R. J.; Fann, Y. C.; Surerus, K. K.; Werst, M. M.; Musser, S. M.; Doan, P. E.; Chan, S. I.; Fee, J. A.; Hoffman, B. M. *J. Am. Chem. Soc.* **1993**, *115*, 10888.

(26) Farrar, J. A.; Neese, F.; Lappalainen, P.; Kroneck, P. M. H.; Saraste, M.; Zumft, W. G.; Thompson, A. J. *J. Am. Chem. Soc.* **1996**, *118*, 11501.

(27) Neese, F.; Zumft, W. G.; Antholine, W. A.; Kroneck, P. M. H. *J. Am. Chem. Soc.* **1996**, *118*, 8692.

(28) Banci, L.; Bertini, I.; Luchinat, C. *Nuclear and Electron Relaxation. The Magnetic Nucleus-Unpaired Electron Coupling in Solution*; VCH: Weinheim, 1991.

(29) Banci, L.; Pierattelli, R.; Vila, A. J. *Adv. Protein Chem.*, in press.

(30) Pfenninger, S.; Antholine, W. E.; Barr, M. E.; Hyde, J. S.; Kroneck, P. M.; Zumft, W. G. *Biophys. J.* **1995**, *69*, 2761.

(31) Clementi, V.; Luchinat, C. *Acc. Chem. Res.* **1998**, *31*, 351.

(32) Bertini, I.; Bren, K. L.; Clemente, A.; Fee, J. A.; Gray, H. B.; Luchinat, C.; Malmström, B. G.; Richards, J. H.; Sanders, D.; Slutter, C. E. *J. Am. Chem. Soc.* **1996**, *118*, 11658.

(33) Luchinat, C.; Soriano, A.; Djinic, K.; Saraste, M.; Malmström, B. G.; Bertini, I. *J. Am. Chem. Soc.* **1997**, *119*, 11023.

(34) Dennison, C.; Berg, A.; Canters, G. W. *Biochemistry* **1997**, *36*, 3262.

(35) Salgado, J.; Warmerdam, G. C.; Bubacco, L.; Canters, G. W. *Biochemistry* **1998**, *37*, 7378.

(36) Dennison, C.; Berg, A.; De Vries, S.; Canters, G. W. *FEBS Lett.* **1996**, *394*, 340.

(37) Holz, R. C.; Alvarez, M. L.; Zumft, W. G.; Dooley, D. M. *Biochemistry* **1999**, *38*, 11164.

(38) Slutter, C. E.; Gromov, I.; Richards, J. H.; Pecht, I.; Goldfarb, D. *J. Am. Chem. Soc.* **1999**, *121*, 5077.

electronic changes can result from minor axial ligand alterations, an observation consistent with available structural data. These mutants are particularly well suited for paramagnetic NMR experiments, enabling a more detailed study of axial perturbations. Accordingly, we have made a detailed ^1H NMR investigation of Met160Gln TtIICu_A.

Materials and Methods

The soluble Cu_A domain was amplified from *T. thermophilus* genomic DNA using standard polymerase chain reaction (PCR) protocols.³⁹ The wild-type fragment is a truncated form of the original construct (T0) that corresponds to the most proteolyzed form of the *Thermus* Cu_A domain. The DNA construct for this form contains a 10 amino acid truncation compared to the original fragment and has been designated as T10 by Fee et al.⁵⁵ Previously, this form has been referred to as T9 by some of us,³⁸ on the basis of a comparison of the longest N-terminal amino acid sequence from the T0 protein product and N-terminal sequence of the T10 protein product. Importantly, both designations, T9 and T10, refer to the same form. This form has been used to determine the crystal structure of the soluble fragment.¹²

The Met160Gln mutant was built in the original construct. The sense primer contained an *Nde* I site (italicized) and start codon (bold) 5'-CTTCGCTTCATCGCCCATATGGCCTACA-3'. The antisense primer, 5'-TTAGCAGCCGGATCCTCACTCCTCACCACGATCGTCCGAA/CTG/GTTC-3', contained the stop codon (bold), *Bam*H I site (italicized), and Met160Gln mutated codon (boxed). The Met160Gln mutation was added to the truncated N-terminal T9 sequence by relegating the *Avr* II/ *Eco*RI fragment from Met160GlnT0 into the WT T9 construct.³⁹ The mutation was verified with automated DNA sequencing using ABI Prism BigDye cycle sequencing chemistry on an ABI Prism 3700 DNA Analyzer and 3100 Genetic Analyzer (Applied Biosystems, Foster City, CA) at the DNA Sequencing Core Laboratory at the California Institute of Technology. Both strands of the gene were sequenced through the restriction sites to verify that no secondary mutation was incorporated in the selected clone.

Protein solutions (2–3 mM) for NMR experiments were prepared in phosphate buffer at pH 8.0. Samples in D₂O were obtained by repeated exchange with D₂O buffer with use of Centricon filters or by dissolving the lyophilized samples in D₂O.

^1H NMR spectra were recorded on MSL 300, AMX 500, and Avance 800 Bruker instruments operating at 300.13, 500.13, and 800.13 MHz, respectively. T_1 measurements were performed using the nonselective inversion–recovery method.⁴⁰ SuperWEFT experiments were performed

(39) Slutter, C. E.; Sanders, D.; Wittung, P.; Malmström, B. G.; Aasa, R.; Richards, J. H.; Gray, H. B.; Fee, J. A. *Biochemistry* **1996**, *35*, 3387.

(40) Vold, R. L.; Waugh, J. S.; Klein, M. P.; Phelps, D. E. *J. Chem. Phys.* **1968**, *48*, 3831.

(41) Inubushi, T.; Becker, E. D. *J. Magn. Reson.* **1983**, *51*, 128.

(42) Banci, L.; Bertini, I.; Luchinat, C.; Piccioli, M.; Scozzafava, A.; Turano, P. *Inorg. Chem.* **1989**, *28*, 4650.

(43) Slutter, C. E.; Gromov, I.; Epel, B.; Pecht, I.; Richards, J. H.; Goldfarb, D. *J. Am. Chem. Soc.* **2001**, *123*, 5325.

(44) Banci, L.; Bertini, I.; Luchinat, C.; Pierattelli, R.; Shokhirev, N. V.; Walker, F. A. *J. Am. Chem. Soc.* **1998**, *120*, 8472.

(45) Bertini, I.; Fernandez, C. O.; Karlsson, B. G.; Leckner, J.; Luchinat, C.; Malmström, B. G.; Nersissian, A. M.; Pierattelli, R.; Shipp, E.; Valentine, J. S.; Vila, A. J. *J. Am. Chem. Soc.* **2000**, *122*, 3701.

(46) De Beer George, S.; Metz, M.; Szilagyi, R. K.; Wang, H.; Cramer, S. P.; Lu, Y.; Tolman, W. B.; Hedman, B.; Hodgson, K. O.; Solomon, E. I. *J. Am. Chem. Soc.* **2001**, *123*, 5757.

(47) Olsson, M. H. M.; Ryde, U. *J. Am. Chem. Soc.* **2001**, *123*, 7866.

(48) Bertini, I.; Luchinat, C. *NMR of Paramagnetic Molecules in Biological Systems*; Benjamin/Cummings: Menlo Park, CA, 1986.

(49) Solomon, I. *Phys. Rev.* **1955**, *99*, 559.

(50) Bertini, I.; Luchinat, C. *NMR of Paramagnetic Substances*; Elsevier: Amsterdam, 1996.

(51) Kurland, R. J.; McGarvey, B. R. *J. Magn. Reson.* **1970**, *2*, 286.

(52) McConnell, H. M.; Robertson, R. E. *J. Chem. Phys.* **1958**, *29*, 1361.

(53) Bertini, I.; Ciurli, S.; Dikiy, A.; Gasanov, R.; Luchinat, C.; Martini, G.; Safarov, N. *J. Am. Chem. Soc.* **1999**, *121*, 2037.

(54) Kalverda, A. P.; Salgado, J.; Dennison, C.; Canters, G. W. *Biochemistry* **1996**, *35*, 3085.

(55) Bertini, I.; Ciurli, S.; Dikiy, A.; Fernandez, C. O.; Luchinat, C.; Safarov, N.; Shumilin, S.; Vila, A. J. *J. Am. Chem. Soc.* **2001**, *123*, 2405.

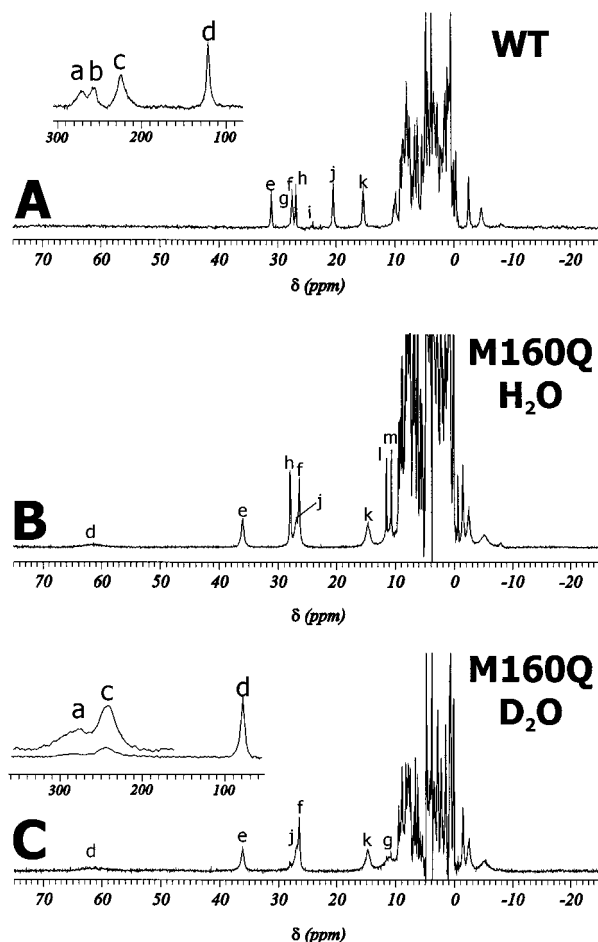


Figure 2. ^1H NMR spectra recorded at 800 MHz, pH 7.0, and 308 K in 100 mM phosphate buffer of (A) WT *T. thermophilus* Cu_A fragment in H₂O (the inset shows the most downfield region with the β -CH₂ signals); (B) Met160Gln mutant in H₂O, pH 8.0; (C) Met160Gln mutant in D₂O, pH 8.0 (the inset shows the most downfield region with the β -CH₂ Cys signals, recorded at 318 K).

according to standard procedures.⁴¹ 1D NOE difference spectra were obtained as described previously.⁴² Exponential and Gaussian weighting functions were used in the spectral processing.

Results

The wild-type (WT) form and Met160Gln mutant of the Cu_A-containing soluble fragment of *T. thermophilus* (TtIICu_A) cytochrome *ba*₃ were expressed in *E. coli* and purified by published methods.^{38,39} The proteins used in this study correspond to the most proteolyzed form of the original *Thermus* construct (see Materials and Methods). Deletion of this N-terminal portion removed a solvent accessible histidine residue, significantly lowering the binding affinity of an additional type 2 copper equivalent that alters the X-band EPR spectra, giving the axial spectrum⁴³ a rhombic appearance.³⁸ The electronic,^{38,55} EPR,^{38,43} and ENDOR⁴³ spectra of the truncated WT fragment have been reported.^{43,43}

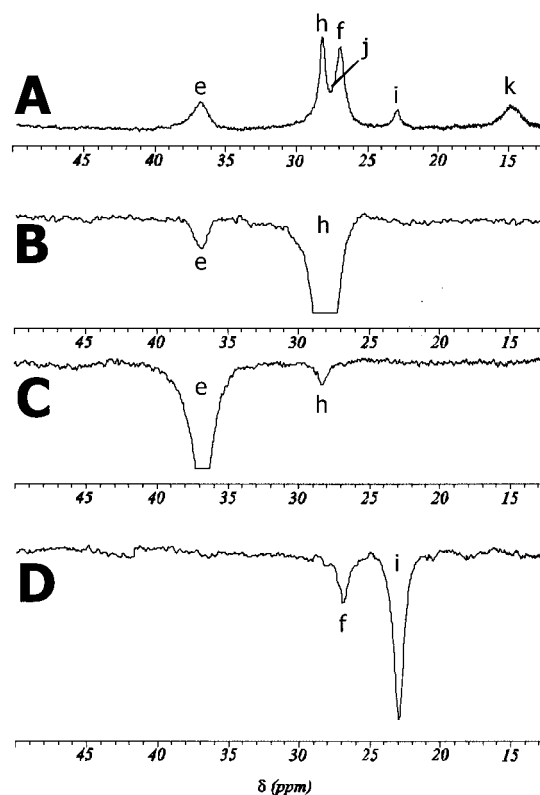
We recorded the ^1H NMR spectra of both the wild-type and Met160Gln proteins (Figure 2). The NMR spectrum of the truncated WT protein is identical to that reported by Bertini et al. for the complete fragment.³² As confirmed by 1D NOE experiments, the signal assignments, as well as the temperature dependences of the hyperfine shifted signals (not shown), are the same as before. We therefore conclude that N-terminal truncation does not alter the NMR properties of the soluble fragment.

Table 1. Spectral Parameters and Assignments of the Hyperfine-Shifted Signals of the Met160Gln TtIICu_A Fragment at 298 K and pH 8.0, unless Indicated^a

signal	δ (ppm)	T_1 (ms)	T -dependence	assignment
a	308	<0.1	hyper-Curie	H β 2 Cys149
c	262	<0.1	hyper-Curie	H β 1 Cys149
d	61	<0.1	anti-Curie	H β 1 Cys153
e	36.9	6.2	Curie	H δ 2 His114
f	27.0	4.3	Curie	H δ 2 His157
g	11.0	n.d.	non-Curie	H α Cys153
h	28.4	n.d.	Curie	He2 His114
i	23.2 ^b	n.d.	Curie	He2 His157
j	26.9	1.2	Curie	He1 His114
k	14.9	0.6	Curie	He1 His157

^a Signal labeling is identical with that used for the WT fragment in ref 32. Residue numbering is that of the full fragment in subunit II.

^b Measured at pH 5.5.

**Figure 3.** (A) ^1H NMR spectra recorded at 500 MHz, pH 5.5, and 298 K in H_2O of Met160Gln. NOE experiments obtained by irradiation of (B) signal e, (C) signal f, and (D) signal i.

The signal pattern in the Met160Gln-TtIICu_A (Figure 2) is characteristic of mixed-valence binuclear [$\text{Cu}^{1.5+}$, $\text{Cu}^{1.5+}$] systems. Two sets of signals are clearly seen in the NMR spectra of Cu_A centers: a first group of sharp, well resolved hyperfine-shifted signals in the 40 to -10 ppm range and a second group of broader lines, with chemical shifts that span 450–60 ppm.^{32–37} These two regions are readily recognized here (the broadest resonances being located in the inset). The T_1 values of the signals in the 15–40 ppm region for the mutant are in the 0.6–6 ms range (between 2 and 17 ms in WTCu_A); those associated with the broader signals a–d are shorter than 1 ms in both proteins. The resonances in the spectrum of Met160Gln mutant are broader than those for the WT protein, and they exhibit shorter T_1 values (cf. Table 1).

An additional exchangeable signal (labeled i) is located in the spectrum at low pH in H_2O (Figure 3A). In the NMR spectra recorded in D_2O solution, the hyperfine signals h, i, l, and m

are absent (Figure 2C). Because only two histidine residues reside at the Cu_A site, two of the signals are likely due to exchangeable imidazole NH protons of these ligands. Signals h and i are the obvious candidates, because their chemical shifts are in the range expected for copper-bound His residues. 1D NOE experiments reveal that WT signal i is dipole-coupled to signal f and signal h is dipole-coupled to signal e (Figure 3). Because the His ligands are bound to the copper through N δ 1 atoms, the following assignments can be made: resonances h and i to the imidazole He2's and e and f to the vicinal H δ 2's. The remaining exchangeable signals (l,m) are likely due to backbone N–H protons in close proximity to the Cu_A cluster. These resonances also are present in the spectrum of the WT protein.³²

No additional dipolar connectivities could be detected between the exchangeable He2's and other hyperfine shifted signals. Signal k is a good candidate for a He1 His, according to its temperature dependence (see later), chemical shift, and shorter T_1 value. The second He1 signal could be buried in the diamagnetic envelope, as in the spectra of the Cu_A domains from *Paracoccus denitrificans* and *Paracoccus versutus*.^{33,35} Another possibility is to assign resonance j, overlapped with signal f, to the remaining He1 proton. Selective irradiation of this signal could not be accomplished because of signal overlap. The assignment of resonances j and k as He1 His is consistent with the presence of these signals in the 60/15 ppm region in the spectra of other Cu_A centers.^{32,33,35}

Signal i is not found in spectra recorded at pH values above 6.0 in H_2O , but it gains intensity at lower pH. Instead, signal h is present in a broad pH range (4.5–8.0). This observation allows a sequence-specific assignment of the His signals, because His157 is solvent-exposed, whereas His114 is not.¹² Therefore, signals i and f are attributed to His157, whereas resonances h and e are assigned to His114.

Three downfield-shifted signals labeled a, c, and d (see discussion below) exhibit shifts and line widths typical of β -CH₂ protons of a S γ -coordinated Cys residue and, hence, can be assigned accordingly. This assignment has been confirmed by Bertini et al. for the WT protein by selective deuteration of the β -CH₂ protons.³² Only three out of four Cys β -CH₂ resonances were detected in the spectrum of the Met160Gln mutant; these fall at 308, 262, and 61 ppm (at 298 K) and are labeled a, c, and d, respectively (see below). Experiments performed with a spectral window as large as 1000 ppm were not helpful in finding the missing signal. Irradiation of resonances a and c was attempted despite their line widths, but the experiment did not yield any NOEs.

The temperature dependences of the ^1H hyperfine shifts of the Cys β -CH₂'s of the WT and Met160Gln proteins are shown in Figure 4. None of the ^1H Cys signals intercepts zero in the linear inverse temperature plots, thus deviating from Curie behavior. Traditionally, the temperature dependences of the hyperfine shifts have been classified as Curie, non-Curie, and anti-Curie. A recent and arguably more precise classification refers to these dependences as Curie, hyper-Curie, and hypo-Curie.⁴⁴

The Cys signals are labeled as in the WT protein, on the basis of similar temperature behaviors and shifts. A clear anti-Curie temperature dependence is observed for signal d in both proteins, the slope in Met160Gln being less pronounced than in WT (Figure 4). Signals a and c exhibit hyper-Curie behavior (i.e., negative intercepts at infinite temperatures). The missing resonance in Met160Gln is thus tentatively attributed to the same

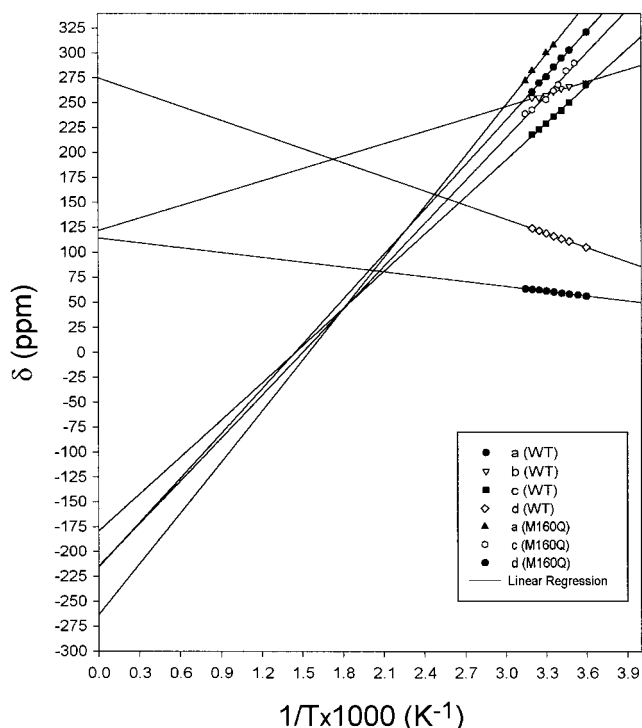


Figure 4. Curie plots of the measured chemical shifts for the β -CH₂ Cys resonances of Met160Gln and WT TtIICu_A.

proton (resonance b) that shows hypo-Curie temperature dependence in the WT protein.

Resonance g at 11 ppm corresponds to a nonexchangeable proton that can be better detected in spectra recorded in D₂O (it is absent in the WT protein). Temperature-independent behavior of the shift of this resonance has been found for H α Cys.^{32,33,33} Because this signal shows a dipolar connectivity with resonance d (not shown), attributed to a Cys β -CH₂, we assign it to H α Cys.

Discussion

The NMR spectrum of the Met160Gln mutant resembles that of the WT protein and of other Cu_A centers (Figure 2), indicating that [Cu^{1.5+}, Cu^{1.5+}] mixed-valence character is preserved, as has been shown by electronic absorption and EPR spectra.³⁸ Differences in the Cys and His signals are not unlike those reported previously from investigations of the NMR spectra of Cu_A centers from different sources.^{32,33,35} In the discussion that follows, we will connect these differences to electronic structure perturbations in the mutant protein associated with axial ligand substitution (Met-to-Gln).

No signals from the axial ligands (Gln160 nor Gln151) could be found outside the diamagnetic envelope in the Met160Gln spectrum, in accord with observations made for the native Met ligands in all Cu_A centers studied hitherto by NMR.^{32,33,35} This means that no net electron spin density is delocalized to the hydrogen nuclei of the engineered Gln, even if a shorter ligand–metal bond is expected compared to Cu–S⁰(Met160). This does not necessarily imply that the Gln(O⁶)–Cu_i bond is weaker than Met (S⁰)–Cu_i in the WT protein. A similar situation is seen in the blue copper protein stercyanin: notwithstanding the stronger interaction of Cu(II) with the Gln axial ligand, no net electron spin density was reported by the Gln protons.⁴⁵ In addition, it should be kept in mind that electron delocalization in Cu_A centers is largely confined to the *xy* plane, and the orbital contribution of axial ligands to the HOMO is small.^{1,27,46,47}

Met160Gln T_1 and T_2 values are in the same range as those of the WT protein, but they are systematically shorter. Nuclear relaxation is controlled by electronic relaxation (τ_s) that dominates the total correlation time.⁴⁸ The longitudinal relaxation of the H δ 2 and He2 His signals is dipolar in origin and, thus, is determined by the value of τ_s and the metal–nucleus distance.³⁴ By using the Solomon–Bloembergen equation, τ_s values of 2×10^{-11} s (WT) and 5×10^{-11} s (Met160Gln) are estimated.⁴⁹

Chemical Shift Analysis. The chemical shifts of the assigned signals can be employed to calculate the unpaired spin density on the metal ligands. The observed chemical shifts are the result of additive contributions of three terms:^{48,50}

$$\delta_{\text{obs}} = \delta_{\text{dia}} + \delta_{\text{con}} + \delta_{\text{pc}} \quad (1)$$

where δ_{obs} is the experimental shift, δ_{dia} is the chemical shift of the nucleus in an analogous diamagnetic system, δ_{con} is the Fermi contact shift due to the unpaired electron density on the nucleus of interest arising from electron delocalization, and δ_{pc} represents the pseudocontact shift stemming from the magnetic anisotropy of the unpaired electron residing on the metal ion.

The pseudocontact contribution can be calculated provided the protein structure and the magnetic anisotropy tensor are known, by using the following equation based on a metal-centered approximation:^{51,52}

$$\delta_{\text{pc}} = \frac{\mu_o \mu_B^2 S(S+1)}{4\pi 9kTr^3} (3 \cos^2 \theta - 1)(g_{\text{par}}^2 - g_{\text{per}}^2) \times 10^6 \quad (2)$$

where r is the proton–copper distance and θ is the angle between the metal–proton vector and the magnetic z axis. In Cu_A, the unpaired electron is delocalized over the Cu₂S₂ rhombus, and an estimate of δ_{pc} should consider two-center or four-center point–dipole interactions. Unfortunately, neither the exact orientation of the magnetic anisotropy tensor nor the electron spin density on each copper and sulfur atom is known, thus precluding an accurate calculation of δ_{pc} . Because δ_{pc} in copper centers is sizeably smaller than δ_{con} ,^{34,45,53–55} we will neglect it in our analysis.

Finally, the hyperfine coupling constants (A/h) can be calculated as follows:⁵¹

$$\frac{A}{h} = \frac{1}{2\pi} \frac{\delta_{\text{con}} 3\gamma_N kT}{g_{\text{av}} \mu_B S(S+1)} \quad (3)$$

where γ_N is the nuclear magnetogyric ratio and g is the isotropic g value. The calculated contact shifts, as well as the hyperfine coupling constants, are set out in Table 2 and are compared to those of the WT protein.

His Signals. The chemical shifts for the His imidazole protons in different Cu_A sites have been discussed by Kolczak et al.,⁵⁶ who suggested that the average shift of the H δ 2 and He2 protons can be used as an empirical estimate of electron spin density for a given His ligand.⁵⁶ The parameters are 28.1 (His114) and 25.5 ppm (His157) for the WT protein and 32.6 (His114) and 25.1 ppm (His157) for the Met160Gln mutant. These results indicate that the two His ligands are less alike in Met160Gln than in the WT protein; specifically, the spin density associated with His114 is detectably altered in the mutant, whereas that with His157 is roughly the same. This result is not unexpected, as His114 is bound to the same copper atom as that in

(56) Kolczak, U.; Salgado, J.; Siegal, G.; Saraste, M.; Canters, G. W. *Biospectroscopy* **1999**, *5*, S19–S32.

Table 2. Observed Shifts, Contact Shifts, and Hyperfine Coupling Constants for the His and Cys Ligands of Cu_A Proteins

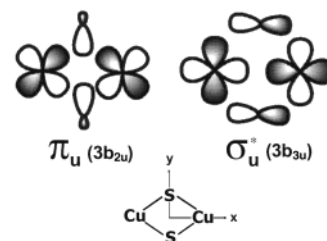
signal	assignment	δ (ppm)	δ_{con}^a	A_c/h (MHz) Met160Gln ^b	A_c/h (MHz) WT ^b	A_c/h (MHz) Paracoccus ^c
a	H β Cys149	308	305	11.38	10.50	10.5
b	H β Cys153			not obsd	9.53	15.0
c	H β Cys149	262	259	9.75	8.90	7.5
d	H β Cys153	61	58	1.87	4.33	2.1
e	H δ 2 His114	36.9	29.9	1.15	0.94	0.76
f	H δ 2 His157	27.0	19.66	0.76	0.77	0.76
g	H α Cys153	11.0	6.4	0.29	0.92	0.74
h	He2 His114	28.4	17.4	0.62	0.51	0.48
i	He2 His157	23.2 ^d	12.16	0.46	0.47	0.58
j	He1 His114	26.9	19.9	0.75	0.53	not obsd
k	He1 His157	14.9	7.9	0.30	0.34	0.41

^a Pseudocontact shifts were neglected (see text). ^b At 298 K. ^c From refs 35 and 54. ^d Measured at pH 5.5.

engineered Gln160 (Figure 1). On the basis of chemical shift similarities of WT and Met160Gln His157 resonances, we suggest that signal k corresponds to the He1 of this residue, whereas resonance j arises from the He1 of His114.

According to Robinson et al., the His imidazole orientations with respect to the Cu_2S_2 rhombus of Cu_A are a function of the distances between the copper atoms and the axial ligands.²³ Our work strongly supports this view: indeed, it is likely that the engineered axial ligand in the mutant affects the copper–His interaction, either by tilting His114 relative to its orientation in the WT protein, or by strengthening the Cu–His bond. Subtle axial ligand differences on Cu_A geometries also are seen by comparison of *Thermus* Cu_A fragment and *ba*₃ oxidase structures. The Cu_A domain, normally packed against subunit I in *ba*₃,⁶ is solvent exposed in the soluble fragment.¹² Interestingly, the Gln151 side chain is fully extended in the *ba*₃ structure, yielding a longer Cu₂–O bond distance. (Cu₁ bond distances are in good agreement in the two structures: this copper is coordinated to Cys149, Cys153, His114, and Met160; distances are 2.4, 2.4, 2.1, and 2.5 Å.) Cu₂ is coordinated to Cys149, Cys153, His157, and Gln151, with distances of 2.3 (2.3), 2.5 (2.3), 2.1 (1.9), and 2.8 (2.6) Å. The distances from the soluble fragment are given in parentheses and, on average, are shorter than those observed for the cytochrome *ba*₃ structure.⁶ The angles between the His114 and His157 imidazole rings differ by one degree, 19° (18°). Both the Cu–Cu [2.4 (2.5) Å] and S–S [4.1 (3.9) Å] distances and the hinge angle 160° (170°) of the core vary. EXAFS studies of the Se-Met160 *Thermus* Cu_A center also have shown a decrease in Cu–Cu distance, 2.43 Å,⁵⁷ without any noticeable changes in EPR or optical spectra compared to the WT Cu_A center. These Cu_A structural studies complement our NMR characterization of the Met160Gln mutant and are consistent with the proposal that axial ligand perturbations of the Cu₁ or Cu₂ coordination environment provide regulatory possibilities that are unique. Importantly, there is compelling experimental evidence that each of the two halves of the Cu_A core can be modulated independently.

Cys Signals. Only three out of four β -CH₂ Cys resonances were located by sampling in a large spectral window, thus suggesting that the fourth was broadened beyond detectable limits. The Cys signal pattern differs from that of the WT protein, showing larger signal spreading (Table 2). Four β -CH₂ Cys signals have been detected in the NMR spectra of the Cu_A soluble fragments from *T. thermophilus* WT,³² *P. denitrificans*,³³ and *P. versutus*.^{35,36} The Cys signal patterns of the two latter

**Figure 5.** Schematic representation of the σ_u^* and π_u orbitals in the xy plane. The orbital labeling according to idealized D_{2h} symmetry (as used in ref 26) is indicated in parentheses.**Table 3.** Cys Dihedral Angles (deg) in Cu_A Proteins

four-atom unit ^{a,b}	WT <i>T. thermophilus</i> ^c	<i>P. denitrificans</i> ^d
	H β –C β –S γ –S γ	
Cys149 H β 1 (c)	–40/–37	–39
Cys149 H β 2 (a)	79/81	79
Cys153 H β 1 (d)	1/9	–10
Cys153 H β 2 (b)	119/128	109
	S–S–C β –C α	
Cys149	–158/–160	–160
Cys153	–112/–120	–131

^a The *T. thermophilus* numbering is used. The corresponding residues in the *P. denitrificans* fragment are Cys 216 and Cys 220. ^b The signal label is indicated in parentheses. ^c From pdb file 2cua.¹² ^d From pdb file 1ar1.¹⁴

proteins are identical, differing from that of the *T. thermophilus* WT protein. The spectral pattern of the Cys residues in Met160Gln resembles more closely those of the Cu_A centers from *P. denitrificans* and *P. versutus*, except for the absence of signal b.

The line widths of signals a, c, and d precluded direct assignments through NOE experiments. However, these signals can be assigned to specific protons on the basis of their positions and temperature dependences. Luchinat et al. have assigned the Cys β -CH₂'s in the *P. denitrificans* fragment from knowledge of the Cu–S–C β –H β dihedral angles,³³ on the basis of a successful application of this approach to rationalize chemical shift variations in iron–sulfur proteins.⁵⁸ The availability of the crystal structure of the TtIICu_A soluble fragment¹² has allowed us to analyze the WT protein data analogously.

The Cys β -CH₂ hyperfine coupling constants follow a sine-squared dependence on the H β –C β –S γ –S γ dihedral angles.³⁵ On the basis of this evidence, Salgado et al. have suggested that the ground state for Cu_A is σ_u^* ,³⁵ in agreement with models proposed by several investigators (Figure 5).^{17,26,27} According to this picture, the S(p) orbitals involved in the HOMO are orthogonal to the sulfur–sulfur vector (Figure 5).

The dihedral angles H β –C β –S γ –S γ (Cys149) are similar in the *Thermus* and *Paracoccus* proteins (Table 3). Signals a and c exhibit similar chemical shifts and a hyper-Curie temperature dependence in both proteins. Thus, we assign these resonances to the β -CH₂ protons of Cys149. The conformation of Cys153 is slightly different (Table 3), consistent with the assignment of resonances b and d to the geminal β -CH₂ couple in the *Paracoccus* and *Thermus* fragments. The different chemical shifts observed for signal b (260 ppm in the *Thermus* protein and 445 ppm in the *Paracoccus* fragments) can be accounted for by consideration of the different dihedral angles (Table 3). An analogous signal could not be found in the spectrum of the Met160Gln mutant.

The less-downfield shifted signal (d), characterized by its anti-Curie temperature dependence, falls at 61 ppm in Met160Gln,

(57) Blackburn, N. J.; Ralle, M.; Gomez, E.; Hill, M. G.; Pastuszyn, A.; Sanders, D.; Fee, J. A. *Biochemistry* **1999**, *38*, 7075.

(58) Bertini, I.; Capozzi, F.; Luchinat, C.; Piccioli, M.; Vila, A. J. *J. Am. Chem. Soc.* **1994**, *116*, 651.

117 ppm in the WT TtICu_A,³² and 55 ppm in the *Paraccocus* fragment.^{33,35} The Cu–S–C_β–H_β dihedral angle spans –10° to 10° in these proteins (Table 3), but such angular variations cannot account for the differences in the shifts (Table 2). In addition, the slope associated with the temperature dependence of signal d in the Met160Gln mutant is half that observed for the WT protein (Figure 4).

The deviations from Curie behavior suggest that one or more excited states are thermally accessible,⁵⁹ as proposed by Salgado et al. in their analysis of temperature dependences of signals in the spectra of Cu_A from *P. versutus*.³⁵ Excessive signal line widths introduce a large uncertainty in the chemical shifts; accordingly, it is difficult to make a reliable estimate of the energy gap between the ground state and the lowest excited state in the case of the Met160Gln protein.

The following qualitative analysis is the best we can do: in the case of Cys153 Hβ1 (d), the S–S–C_β–H_β dihedral angles range from –10° to 9° in the different Cu_A centers, and smaller hyperfine couplings are predicted for the ground state, consistent with a narrower signal (d) at 100–50 ppm. The hyperfine couplings in the π_u excited state, instead, should have a cosine-squared dependence on the S–S–C_β–H_β dihedral angles, thereby giving a significant increase in the hyperfine coupling of Cys153 Hβ1 compared to the ground state. The anti-Curie behavior of resonance d is consistent with this model, because raising the temperature would result in greater π_u population and larger Fermi contact shifts. The smaller chemical shifts observed for signal d, and the smaller slope, suggest that the excited state of Met160Gln is shifted to higher energies compared to that of WT, provided the Cys153 sulfur electron spin density is not substantially altered. This latter possibility can be ruled out, because the hyperfine coupling constants for resonances a and c are less than 10% greater than those of the WT protein.

A larger σ_u*–π_u energy gap in the mutant should shift signal b to a position above that of the WT protein. If this were the case, a broader resonance would be expected, because transverse relaxation rates (and hence, line widths) of methylene Cys protons in blue copper and Cu_A centers are dominated by the contact contribution.^{35,53} Excessive broadening may explain the apparent absence of this signal in the spectrum of the Met160Gln protein.

Our data strongly support the existence of a low-lying excited state in Cu_A centers,³⁵ whose energy is tuned by interactions of the copper atoms with the axial ligands. As noted, this picture is consistent with changes in the electron relaxation time. Recent DFT calculations predict a σ_u*–π_u energy gap smaller than 400 cm^{–1} for Cu–Cu distances in the range observed in the crystal structures.⁴⁷ Several calculations also suggest that changes in the Cu–Cu distance (or in the Cu–S–Cu angle) tune the relative energies of the σ_u* and π_u orbitals.^{17,47,60,61} Specifically, the HOMO is predicted to change from mainly σ_u* to π_u for a Cu–S–Cu angle in the range 67–70°.^{60,61} The Cu₁–S₁₄₉–Cu₂ angle is 62° (65°) and the Cu₁–S₁₅₃–Cu₂ angle is 60° (65°) in the fragment and *ba*₃ Cu_A structures, with the corresponding angles for the fragment given in parentheses. Thus, the adjustments in core geometry for a 0.2 Å change in the Cu₂–O interaction of the Gln151 axial ligand are not expected to alter the ground state. Additionally, ENDOR results for both the Met160Gln and Met160Glu proteins indicate that a σ_u* ground state is retained in these mutants.⁴³ These findings suggest that

minor axial distortions are too subtle to produce a change in ground state. Density functional calculations on hinge angle distortions of the Cu–S core have shown retention of the σ_u* ground state over a large range.⁶¹ As noted earlier, the hinge angle in these structures differs by 10°, a more significant change than that seen in the Cu–S–Cu angles of the core. The hinge angle distortion of the core has received less attention than others; nevertheless, this type of perturbation is consistent with a larger σ_u*–π_u energy gap in the Met160Gln mutant. The energy of π_u is altered by decreasing the hinge angle and, hence, the Cu–Cu distance, thereby tuning the excited state with minimal bond length changes. The σ_u*–π_u gap of Cu_A in the *ba*₃ structure is expected to be greater than in the more flattened core of the soluble fragment.

A good deal of evidence suggests that axial ligand interactions play a role in tuning the electronic structures and the reduction potentials of blue copper proteins.^{62,63} ¹H NMR spectra show that when Met (plastocyanin) is replaced by Gln (stellacyanin) the average hyperfine coupling for the β-CH₂ geminal couple decreases from 20 to 14.5 MHz.⁴⁵ This decrease, which mainly reflects changes in Cys electron spin density, is strikingly different from the present case, in which a similar mutation does not alter substantially the Fermi contact shifts associated with Cys moieties. These observations are in line with those based on other spectroscopic measurements.^{64,65} Strong axial ligands in blue copper proteins induce changes in the relative intensities of LMCT absorptions and give rise to rhombic EPR spectra.^{62,66} In contrast, the LMCT band pattern in Met160Gln–Cu_A is only slightly altered with respect to that of the WT protein, and the EPR spectrum is axial.^{38,43}

The accumulated evidence suggests that the interplay between the Cys₂His₂ ligand set and the axial ligands in Cu_A centers is different from that postulated for the axial-CysHis₂ interaction in blue copper sites. We suggest that axial ligands distort the Cu₂S₂ core rhombus to a conformation with a tunable low-lying excited state that is partially populated at 70 °C, the growth temperature of *T. thermophilus*. It is possible, perhaps even likely, that this state regulates electron transfer in the functioning oxidase.

The four electron reduction of O₂ to water and ET coupling to proton translocation are precisely controlled events.^{67,68} However, there is no consensus on the control mechanisms that coordinate the reaction cycle. Our work on the Met160Gln model system suggests that axial ligands could independently sense cyt *c*₅₅₂ binding and changes at the subunit I/II interface. The backbone of Met160 is solvent exposed in the proposed cyt *c*₅₅₂ binding site.⁶ Conformational changes induced on binding of reduced cyt *c*₅₅₂ can be transmitted to Cu₁. Similarly, changes in the subunit I/II interface can be detected by the Gln151 side chain and transmitted to Cu₂. The advantage of this center is that one or both events could be detected at any given moment in the reaction cycle.

(62) Randall, D. W.; Gamelin, D. R.; LaCroix, L. B.; Solomon, E. I. *J. Biol. Inorg. Chem.* **2000**, *5*, 16.

(63) Gray, H. B.; Malmstrom, B. G.; Williams, R. J. P. *J. Biol. Inorg. Chem.* **2000**, *5*, 551.

(64) La Croix, L. B.; Randall, D. W.; Nersissian, A. M.; Hoitink, C. W.; Canters, G. W.; Valentine, J. S.; Solomon, E. I. *J. Am. Chem. Soc.* **1998**, *120*, 9621.

(65) Vila, A. J.; Fernandez, C. O. *J. Am. Chem. Soc.* **1996**, *118*, 7291.

(66) Lu, Y.; LaCroix, L. B.; Lowery, M. D.; Solomon, E. I.; Bender, C. J.; Peisach, J.; Roe, J. A.; Gralla, E. B.; Valentine, J. S. *J. Am. Chem. Soc.* **1993**, *115*, 5907.

(67) Babcock, G. T.; Wikström, M. *Nature* **1992**, *356*, 301.

(68) Proshlyakov, D. A.; Pressler, M. A.; DeMaso, C.; Leykam, J. F.; DeWitt, D. L.; Babcock, G. T. *Science* **2000**, *290*, 1588.

(59) Shokhirev, N. V.; Walker, F. A. *J. Phys. Chem.* **1995**, *99*, 17795.

(60) Neese, F. Ph.D. Thesis, University of Konstanz, 1996.

(61) Ramirez, B. E. Ph.D. Thesis, California Institute of Technology, 1997.

The more complicated mitochondrial aa_3 oxidases function with up to 10 nuclearly-encoded subunits. These subunits are believed to have regulatory functions; however, only subunit IV has been studied in any detail. ATP binds to the matrix domain of subunit IV and allosterically inhibits oxidase activity. cAMP-dependent phosphorylation of subunits II, III, and Vb has been shown to be a necessary condition for the bovine oxidase to display ATP/ADP-ratio dependent inhibition.^{69,70} A conformational change altering the axial interactions upon phosphorylation and ATP binding to subunit IV could increase the energy of the low-lying Cu_A excited state and inhibit electron injection into the oxidase from reduced cyt *c* at physiologically relevant temperatures. Thus, the excited-state tunability exhibited by Cu_A is ideally suited to the expanded regulatory needs of the mitochondrial oxidases and offers a broader range of regulatory possibilities than would be possible with a simple switching of ground states.

Concluding Remarks

Our NMR study shows that the distinctive purple copper delocalized electronic structure is preserved in the Met160Gln mutant of TtII Cu_A ; what is more, the electron spin density pattern is not severely altered. The observation that the engineered Gln160 induces changes in His114 chemical shifts strongly supports the suggestion that axial ligand interactions

determine the His orientations, and the finding that these minor geometric changes are limited to one copper atom underscores the structural robustness of Cu_A sites, a feature that is crucial in minimizing the reorganization energy while allowing variation in the reduction potential of the center.^{71,72} The interaction with Gln160 apparently does not weaken the Cu–S(Cys) bond as in blue copper proteins. Instead, this perturbation tunes the relative energies of low-lying electronic levels, most probably through minor geometric rearrangements of the binuclear complex. It follows that this fine-tuning could be exploited in the design of highly efficient electron-transfer units.

Acknowledgment. This work was supported by NIH Grants R01-DK19038 to H.B.G. and R01-GM16424 to J.H.R. and FIRCA-NIH Grant R03-TW000985-01 to H.B.G. and A.J.V. C.O.F. and A.J.V. are staff members at CONICET. J.A.C. is recipient of a fellowship from CONICET. We thank Ramiro Rodríguez for help with protein purification and Sergio Dalosto for helpful discussions. C.O.F. and A.J.V. thank CERM (University of Florence) for allowing C.O.F. to record the 800 MHz spectra and for the hospitality offered to C.O.F.

JA0162515

(71) Ramirez, B. E.; Malmström, B. G.; Winkler, J. R.; Gray, H. B. *Proc. Natl. Acad. Sci. U.S.A.* **1995**, *92*, 11949.

(72) Farver, O.; Lu, Y.; Ang, M. C.; Pecht, I. *Proc. Natl. Acad. Sci. U.S.A.* **1999**, *96*, 899.

(69) Bender, E.; Kadenbach, B. *FEBS Lett* **2000**, *466*, 130.

(70) Steenart, N. A.; Shore, G. C. *FEBS Lett.* **1997**, *415*, 294.